NANO LETTERS
pubs.acs.org/NanoLett

Nonlithographic Patterning and Metal-Assisted Chemical Etching for Manufacturing of Tunable Light-Emitting Silicon Nanowire Arrays

Winston Chern,[†,‡] Keng Hsu,[†,§] Ik Su Chun,[†,||] Bruno P. de Azeredo,[†,§] Numair Ahmed,[†,§] Kyou-Hyun Kim,[‡] Jian-min Zuo,[‡] Nick Fang,[*,†,§] Placid Ferreira,[*,†,§] and Xiuling Li[*,†,||,‡]

[†]Center for Nanoscale Chemical-Electrical-Mechanical Manufacturing Systems, [||]Department of Electrical and Computer Engineering, [‡]Department of Materials Science and Engineering, and [§]Department of Mechanical Science and Engineering, University of Illinois, Urbana, Illinois 61822

ABSTRACT Semiconductor nanowires have potential applications in photovoltaics, batteries, and thermoelectrics. We report a top-down fabrication method that involves the combination of superionic-solid-state-stamping (S4) patterning with metal-assisted-chemical-etching (MacEtch), to produce silicon nanowire arrays with defined geometry and optical properties in a manufacturable fashion. Strong light emission in the entire visible and near infrared wavelength range at room temperature, tunable by etching condition, attributed to surface features, and enhanced by silver surface plasmon, is demonstrated.

KEYWORDS Silicon nanowire, metal-assisted-chemical-etching (MacEtch), S4, light-emitting, sidewall roughness

High-aspect ratio semiconductor nanostructures have started to have a profound effect on the design and performance of many types of devices, including batteries, solar cells, detectors and thermoelectric systems. For example, it has been demonstrated recently that using silicon (Si) nanowires as the anode in a lithium battery could enhance the battery charge capacity and promote a longer battery life.[1] This is attributed to the large strain accommodation capacity of the nanoscale dimension thus resilience to pulverization upon lithium insertion and extraction, and efficient one-dimensional carrier transport along the nanowires. For thermoelectric applications, a 100-fold reduction of thermal conductivity has been found in rough Si nanowires leading to an enhanced figure-of-merit ZT of 0.6 at room temperature.[2,3] Using Si nanowire arrays for solar cell applications has also been demonstrated with promising results, owing to the high antireflectivity hence better absorption efficiency.[4−7]

To produce high-aspect ratio silicon nanowire arrays, either a bottom-up growth method through metal-catalyzed vapor−liquid−solid (VLS) mechanism[8] or a top-down method through lithography and etching can be used.[9,10] In the VLS method, diameter and position can be controlled in principle by catalyst and impressive uniformity and density have been demonstrated. This bottom-up paradigm generates nanowires with smooth sidewalls with no active light-emitting properties and requires a growth chamber and growth condition that ensures epitaxial growth towards desired orientations on appropriate substrates.

Light emission from porous silicon structure due to quantum confinement was first discovered by Canham in 1990 and emission in the entire visible as well as UV range is of interest for various applications.[11] Blue and UV Si emission can be generated through sonication of porous silicon and immersion in HF and H_2O_2 for several hours to generate small discrete nanoparticles.[12] Highly controllable photoluminescence has also been reported for Si-rich SiO_2 layers that are formed using reactive ion sputtering.[13,14] Recent innovative techniques such as the cooling of laser ablated Si in supercritical CO_2 and metal-assisted chemical etching have also been applied to produce blue and other visible emissions.[15,16] Nanoparticles, dispersed via a colloidal solution and electroplated on appropriate substrates, have found applications as the active layer of devices such as UV detectors.[17] It is desirable to have a method that can produce tunable light emission/absorption in a broad range of the spectrum from IR to UV in a manufacturable fashion.

Here we present a top-down scalable nanofabrication method for production of three-dimensional (3D) silicon structures that are versatile in geometry and properties. This method combines two high-throughput parallel fabrication techniques, superionic solid state stamping (S4)[18,19] and metal-assisted chemical etching (MacEtch).[20] It provides a viable path for wafer scale manufacturing of 3D functional semiconductor nanostructures with lateral resolutions as small as 10 to 100 nm and extremely high aspect ratio that

* To whom correspondence should be addressed. E-mail: (X.L.) xiuling@illinois.edu; (P.F.) pferreir@illinois.edu; (N.F.) nicfang@illinois.edu.
Received for review: 11/16/2009
Published on Web: 04/27/2010

© 2010 American Chemical Society

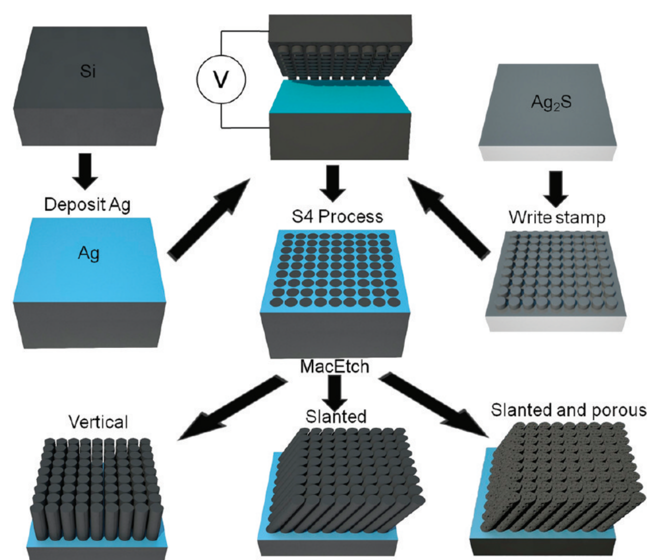

FIGURE 1. S4 and MacEtch Process flow. Schematic diagrams illustrating the process of using stamps written from Ag_2S (right) to pattern deposited Ag film on silicon wafer (left) for superionic solid state stamping (S4) of Ag patterns (middle), followed by MacEtch, which yields solid silicon nanowires in vertical or slanted configuration as well as porous and slanted nanowires (bottom row), depending on etching conditions.

is limited mainly by etching time.[21−23] Red-green-blue emissions from silicon nanowire arrays are produced and tunable through the control of a variety of parameters including MacEtch solution concentration, etching time, silicon wafer crystal orientation and doping, and metal catalyst type. The capability of this method could potentially open new design possibilities such as high efficiency all-silicon tandem solar cell consisting of Si nanowires monolithically stacked to absorb different parts of the solar spectrum.[24,25]

Figure 1 illustrates the process flow for the combined S4-MacEtch fabrication method (see Methods for details). Figure 2 shows several different types of 3D silicon nanostructures fabricated from two-dimensional Ag patterns generated using S4 stamping followed by MacEtch. They include the conversion of metallic Ag dots on Si surface to vias in silicon (Figure 2a−c); closely packed arrays of 1 μm × 1 μm Ag squares on silicon surface to silicon grids (Figure 2d−f); concentric Ag rings to multilayer annular silicon shells (Figure 2g−i); and Ag mesh pattern on silicon surface to silicon nanowire array (Figure 2j−l). These results fully demonstrate that S4-MacEtch can engrave the two-dimensional metal pattern, whether it is linear or circular, discrete or interconnected, to create 3D high aspect ratio silicon nanostructures.

The essence of MacEtch is that nanoscale metallic patterns formed on top of a semiconductor surface can be transferred into the semiconductor body when exposed to a solution that contains an oxidant (e.g., hydrogen peroxide (H_2O_2) or nitric acid (HNO_3)) and hydrofluoric acid (HF).[20,10] The metal acts as a local cathode and a catalyst to promote the reduction of the oxidants and generates free holes (h^+) at the metal−semiconductor interface. As a result, the

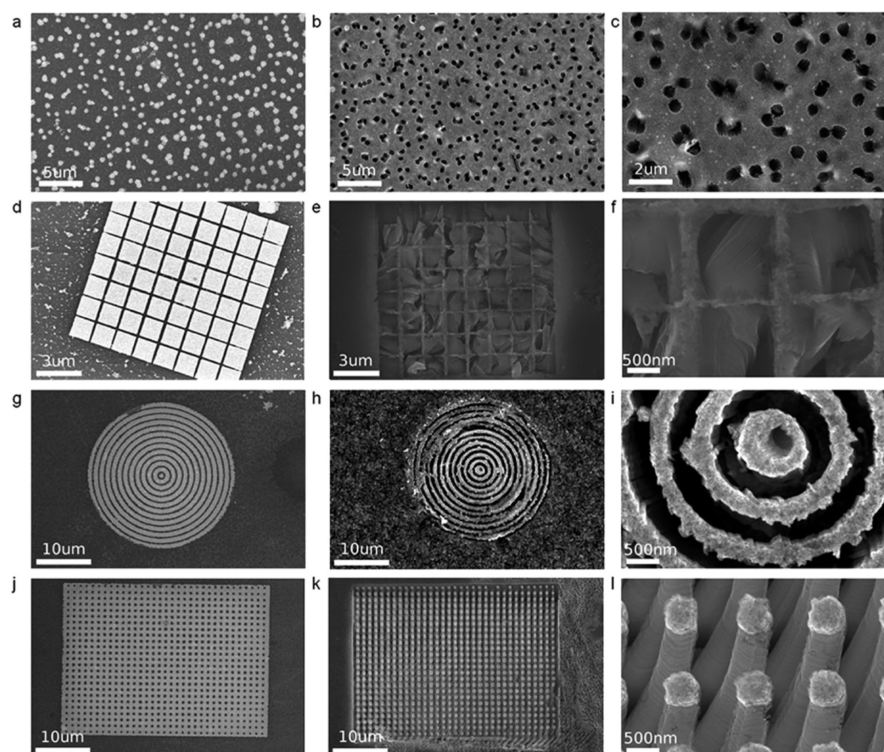

FIGURE 2. S4 and MacEtch generated three-dimensional Si nanostructures: Ag patterns generated by S4 (a,d,g,j); corresponding sets of Si structures shown at two different magnifications after subsequent MacEtch for 3 min ((b,c), (e,f), (h,i)) and 6 min (k,l).

© 2010 American Chemical Society

DOI: 10.1021/nl903841a | *Nano Lett.* **2010,** *10,* 1582--1588

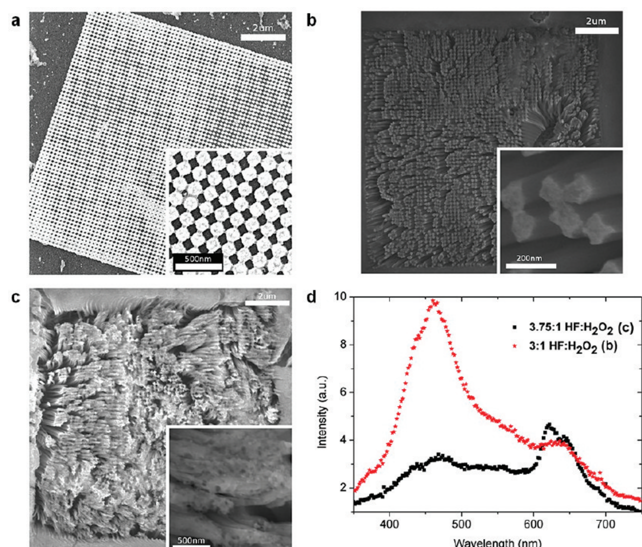

FIGURE 3. Effect of etchant concentration on nanowire orientation, morphology, and optical properties. SEM images of the S4 printed Ag pattern on p-type Si (100) wafer (a) after MacEtch for 3 min in 3:1 (b) and 3.75:1 (c) HF/H_2O_2 solution. Insets show higher magnification images. (d) CL spectra taken from sample (b) and (c) as indicated, where the solid vertical wires (b) show strong blue (∼470 nm) emission, while porous slanted wires (c) show weaker total emission with stronger emission in the red (∼624 nm) than blue wavelength.

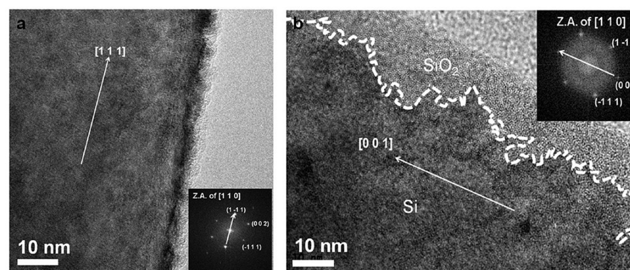

FIGURE 4. High-resolution TEM images with corresponding FFT patterns along [110] zone axis, indicating the nanowire axial directions as ⟨111⟩ and ⟨100⟩ for (a) and (b), respectively. These silicon nanowires are formed by MacEtch of Si (100) wafer at different etching conditions listed in Table I. The interface between silicon and the amorphous oxide layer is traced with dashed lines for the (100) nanowire for visual clarity. See text for discussion of nanoscale surface roughness.

material directly underneath the metal is preferentially removed under controlled etching and appropriate selection of metal. The metal travels downward as the semiconductor is removed beneath it, maintaining a metal−semiconductor junction and enabling continuous etching under the catalyst metal.

Silicon etching can be achieved through MacEtch regardless of the doping type and level with varied etch rate and geometry.[20] The depth of the etched features is controlled by etching time. The generated holes (h^+) follow two different routes: they are either consumed right away by reacting with the silicon in immediate proximity (resulting in the removal of silicon directly in contact with the metal) or diffuse out before reaction (resulting in porous region off the metal). Thus the final silicon nanostructure generated can be controlled by the type of metal (Ag, Au, Pt, etc.),[26] the metal feature size and spacing, the etchant concentration ($H_2O_2/(HF + H_2O_2)$),[27] substrate doping type, level,[28,29] and crystal orientation.[29]

The ratio of HF to H_2O_2 in the MacEtch solution affects both the etching direction and wire morphology. Shown in Figure 3 are the MacEtch results for S4 generated Ag patterns under different MacEtch etching concentrations for p-type (100) silicon wafers with resistivity of 6−8 Ω·cm. Vertical nanowires are formed at HF/H_2O_2 ratios less than 3:1 while slanted nanowires are generated when the HF ratio is increased beyond 3:25:1. In all case, the volume of EtOH equals to that of 49% HF used and is not noted explicitly. In addition to the difference in directions, the variation of morphology of the nanowires is also evident. The vertical nanowires in this case appear to be solid while the tilted ones are porous (see high-magnification SEM images in the inset of Figure 3). Table I summarizes the dependence of nanowire orientation and morphology on substrate crystal orientation and etching condition, as well as the process window. The vertical nanowires are defined as those oriented along the surface normal, that is, vertical wires on (100) surface are [100], on (110) surface are [110], and so forth. While for the slanted nanowires, the slanting angles relative to the wafer surface differ depending on the etching condition. Note that ⟨111⟩ is 35.3° slanted from the (100) surface, slanted by 54.7° from the (110) surface, and slanted by 19.5° from the (111) surface. The orientations listed in Table I are the best identification based on nanowire angles estimated from SEM images. Figure 4 show two examples of the nanowires with confirmed orientations by TEM selected area electron diffraction patterns. The [111] and [100] nanowires in Figure 4a,b are formed using etching conditions corresponding to those in Table I row 1 column 5 and column 3, respectively. The [100] nanowire imaged here is the same as those in Figure 3b. It is evident that the [100]

TABLE I. Dependence of Si Nanowire Direction and Morphology on S4−Ag MacEtch Condition and Si Wafer Surface Orientation[a]

	concentration (HF/H_2O_2 volume ratio)						
	<<1:1	1.5:1−2:1	2.5:1−3:1	3:1−3.25:1	3.25:1−3.5:1	3.5:1−4:1	>>4:1
(100) Si wafer	no pattern	porous vertical <100>[27,28]	vertical <100>[27,29]	slanted <110>	slanted <111>	porous slanted <111>	no pattern
(110) Si wafer	*no pattern*	*porous slanted <100>*	*slanted <100>*	vertical <110>	slanted <111>	porous slanted <111>	*no pattern*
(111) Si wafer	*no pattern*	*porous slanted <100>*	*slanted <100>*[29]	slanted <110>	vertical <111>	*porous vertical <111>*	*no pattern*

[a] Non-italic fonts represent direct observations from this study and italic fonts represent projected properties. Consistent literature reports are indicated wherever available.

© 2010 American Chemical Society

DOI: 10.1021/nl903841a | Nano Lett. 2010, 10, 1582–-1588

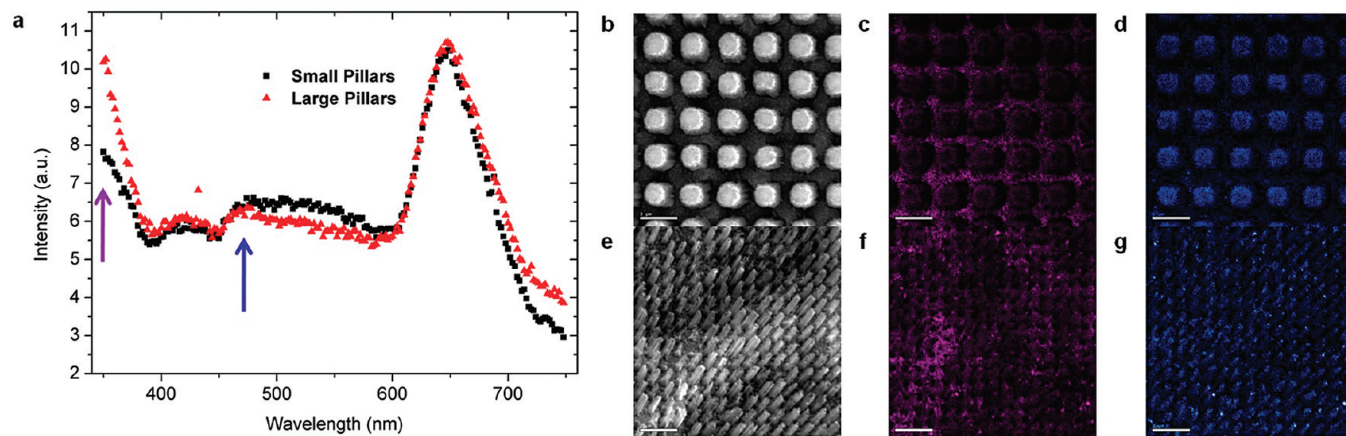

FIGURE 5. CL spatial correlation. CL spectra (a) taken from two sets of silicon pillars shown in SEM images (b) and (e); faux color CL images taken at 350 nm ((c) and (f)), and at 470 nm ((d) and (g)), indicated by like-color arrows in (a), for the corresponding pillar structure. The scale bars represent 2 μm.

nanowire has an extremely rough interface between silicon and the amorphorous layer, presumably silicon oxide. The height variation on surface is as much as ~12 nm and lateral undulating features are as small as ~1 nm. Nanowire orientations and porosity produced by MacEtch in literature reports are also consistent with Table I results and projected properties where available.[27-29]

We attempt here to explain the nanowire orientation based on the MacEtch mechanism.[20,29] At low [HF]/[H_2O_2] ratio, that is, high relative H_2O_2 concentration, holes (h^+) are readily generated at the cathode (Ag) to oxidize Si to Si^{4+}, but HF is not readily available to remove the silicon. Therefore, it is conceivable that the etching would occur in the least compact crystal direction, ⟨100⟩, where there are the fewest surface atoms to remove. As the number of holes (h^+) becomes more limited at high [HF]/[H_2O_2] ratio, the removal of Si^{4+} will become quicker due to a higher relative concentration of HF leaving less time for hole diffusion resulting in etching in a direction with more surface atoms such as ⟨110⟩ and ⟨111⟩. As for the morphology (nonporous vs porous) evolution with etching concentration, it seems that solid nonporous wires can only be produced when the HF and H_2O_2 concentrations are somewhat balanced and beyond that window on both sides of the concentration chart, porous structures are generated. Porous nanowire structures form because of hole (h^+) diffusion beyond the metal-semiconductor interface. Our observations imply that both excess hole (h^+) generation (high H_2O_2 concentration) and high rate of Si^{4+} removal (high HF concentration) allow hole (h^+) diffusion to areas that are between the patterned metal. For different geometry, size, doping type and concentration, and metal catalyst type, the etching parameter space for the defined orientation and porosity may shift, but the trend should remain the same. Recently, it was reported that a change in nanowire porosity has been observed as a function of silicon doping concentration while maintaining the MacEtch concentration.[3,28] Whether increasing doping concentration or decreasing the relative concentration of HF/H_2O_2, the essential change is the amount of carriers (h^+) injected and consumed that regulates both the porosity and etching direction.

In general, we have observed strong emissions in the entire visible and near infrared range at room temperature from various S4-MacEtch-produced silicon nanostructure arrays. However, the overall emission intensity and relative intensity in different wavelength range vary depending on the structures produced using different etching concentration, etching time and patterns. Shown in Figure 5a are CL spectra taken from two sets of nanowire arrays directly after MacEtch (i.e., the Ag metallic pattern remains in the body of silicon). The CL spectra indicate strong emission in the UV region near 350 nm, a strong peak in the red at ~648 nm, and a broad band in other visible color range. Using monochromatic CL images taken at each wavelength window (Figures 5c,d, and 5f,g) and comparing with the corresponding SEM images (Figure 5b,e), we have unambiguously identified that the emission at 350 nm originates from the Ag pattern (bulk plasmon between wires (Figure 5c,f), while the emission in the blue ~470 nm (Figure 5d,g), green, and red (not shown) comes from the silicon nanowires themselves. Surprisingly, the two sets of nanopillars with diameters at 400 and 1000 nm show amazingly similar emission wavelength and intensity. It is however not completely unexpected considering that the diameter range studied here is well above the quantum confinement threshold (exciton Bohr radius for silicon is 5 nm), and the visible emission observed here most likely originates from surface features produced as a result of S4-MacEtch.

Remarkably, the relative intensity in each color band as well as the overall intensity can be tuned by varying etchant concentration, etching time, silicon substrate properties (orientation, doping concentration) as well as the type of catalyst metal. As shown in Figure 3d, for MacEtch under 3.75:1 [HF]/[H2O2] condition for 3 min, the dominant CL peak is ~624 nm (red color) with a broad band that covers between 400−600 nm, while reducing the [HF] concentra-

© 2010 American Chemical Society

DOI: 10.1021/nl903841a | Nano Lett. 2010, 10, 1582--1588

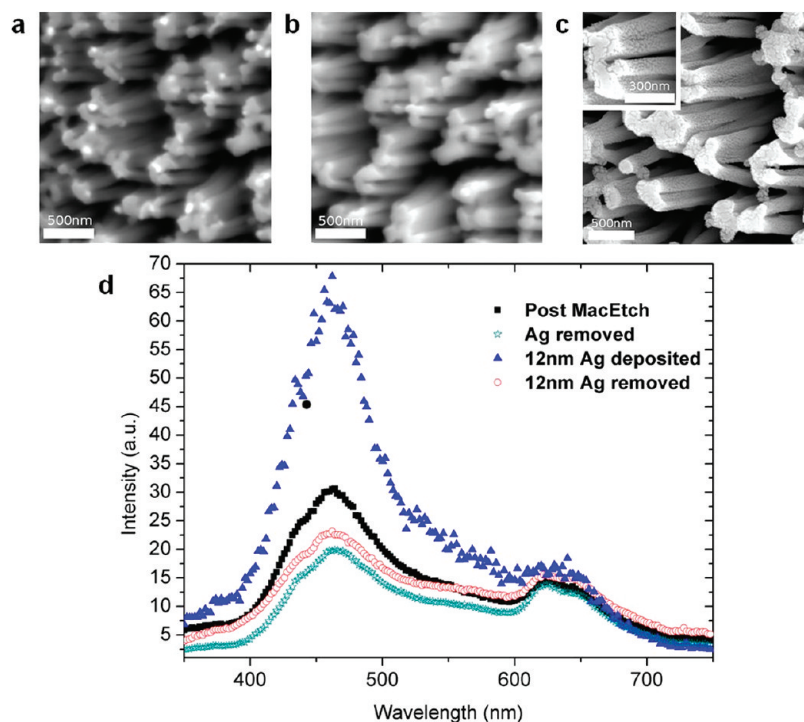

FIGURE 6. Surface plasmon enhancement. CL spectra (d) taken directly after MacEtch (SEM image (a) showing bright metallic tips at the top of the nanowires), after Ag is removed (SEM in (b)), after intentional redeposition of 12 nm (nominal thickness) of Ag film (SEM (c) showing grainy Ag nanoparticles), and after the removal of Ag again.

tion by 20% to 3:1 [HF]/[H2O2], increases the blue emission ~470 nm by more than 3 times. In addition to concentration, increasing etching time from ~30 s to >3 min has shifted the emission from red to blue color (not shown), consistent with previous reports on wavelength shift but on a much faster time scale.[10,17] Careful examination of the morphology of the nanowire sidewalls and top surface indicate that the surface becomes rougher with increasing H_2O_2 concentration or etching time. Solid nanowires with nanometer scale rough surface features (Figure 4b) correspond to dominantly blue emission, while milder height undulation (Figure 4a) or porous type of nanowires (Figure 3c) emit in the red and near IR wavelength range. Red emission has been reported from MacEtch produced porous silicon nanowires.[27,28]

It is important to point out that MacEtch is normally confined at the metal semiconductor interface level. Thus the resulting silicon nanostructure should not experience further etching while metal continues to sink in, which is the argument for high-aspect ratio vertical wall features without undercutting.[10,30] However, it is known that metallic Ag can be etched by HF and H_2O_2 solutions. Yet in the case of MacEtch, it appears that most of the Ag pattern remains on silicon surface, presumably because etched silver in the form of Ag^+ can be reduced by Si back to Ag when it is in direct contact with silicon, preventing it from being fully dissolved.[29] To test this hypothesis, a 5 nm Cr adhesion layer was deposited between silicon surface and the Ag layer. This resulted in the Ag layer being completely etched away with a smooth Cr film remaining on the surface. Silicon etching stopped at that point since Cr does not act as a catalyst in MacEtch, and Ag in solution did not cause silicon etching. This confirms that the intimate contact relationship between catalyst metal and the semiconductor is essential in MacEtch. Even though there is no net consumption of Ag, some Ag particles could reside on the nanowire sidewalls and top surfaces randomly and MacEtch continues locally increasing the sidewall roughness overtime. In contrast, samples etched using inert metals as the catalyst, such as Au or Pt, have not been seen to possess blue emissions.[10,20]

The Ag S4-MacEtch produced nanowire arrays reported here resulted only from 3 min etching with dominantly blue emission, which is much shorter in contrast to blue color emission reported in porous silicon generated by both traditional anodic etching and broad area Ag catalyzed MacEtch (45 and 10 min required, respectively).[16,31] Furthermore, this is the first report on blue emission from ordered silicon nanowire arrays. Overall, etching conditions and silicon surfaces determine the structure of the nanowires that in turn affect the optical properties. This provides unique tunability of light emission from silicon, an elemental indirect band gap semiconductor, with unprecedented control of its optical properties through nanofabrication.

The other unique feature about Ag S4-MacEtch silicon structures is the plasmonic coupling effect due to the presence of Ag nanoparticles, which could selectively enhance certain wavelength range of the nanowire emission. Shown in Figure 6d are CL spectra taken from the same sample

© 2010 American Chemical Society

DOI: 10.1021/nl903841a | Nano Lett. 2010, 10, 1582--1588

undergone cycles of Ag deposition and removal after the silicon nanowires are formed. The black-colored CL trace is taken directly after MacEtch while residual Ag particles remain on the tip and sidewalls of the nanowires. The cyan color trace is after the removal of the Ag particles from the nanowire sample by chemical etching. Clearly, the peak intensity in the blue wavelength range shows a decrease by a factor of ~1.7, while not much change is observed in the red wavelength range. The presence and the absence of Ag can be viewed from SEM images (Figure 6a,b) as well as CL images as local bright spots. Next, we have intentionally redeposited an Ag metal film of 12 nm nominal thickness (resulting in discrete grainy Ag nanoparticles of ~50 nm or less in size, as shown in the SEM image in Figure 6c), which leads to a dramatic enhancement of the blue peak at 470 nm (blue color trace) by ~4 times. The blue wavelength emission intensity has subsequently been returned to the original level once the Ag is etched off (red color trace). This series of experiments has unequivocally confirmed a strong enhancement of the blue emission due to the presence of Ag nanoparticles. We attribute such enhancement to Ag surface plasmon resonance on silicon, and the roughness of the silicon film is essential for light extraction. This is consistent with a recent report where Ag film strongly enhanced blue emission from InGaN/GaN quantum well surface at ~410 nm.[32] To the best of our knowledge, this represents the first report on plasmon enhancement of light emission from silicon nanowires. We foresee that by tailoring the metal particle type, size, and pattern, it should be possible to selectively enhance the emission of certain wavelength quantitatively to provide a strongly tunable light emitting or absorbing source in the entire visible range.

Conclusions. By combining S4 stamping and MacEtch, we have introduced a simple, high-throughput method of generating many different 3D patterns in Si in a manufacturing fashion. Yet, the process is versatile and by controlling the etching concentration, time, silicon surface orientation, and doping properties, patterns with the desired crystal orientation and optical properties can be produced. The control of the crystal orientation can be used for changing the reflectivity of silicon[33] and the porosity can be used to vary the dielectric constant, strain accommodation capacity, as well as quantum-confined band structure. The unprecedented tunability of light emission in the entire visible wavelength range through nanofabrication, from an indirect bandgap elemental semiconductor with dimensions well above the Bohr radius, could lead to many applications including silicon nanowire based tandem solar cells. Further plasmonic enhancement has outlined a possibility to locally enhance absorption in selected wavelength range for better detectors and photovoltaics.

Methods. MacEtch is a simple, fast, and effective formation method for nanostructured semiconductors, where selective removal of the semiconductor is assisted by metal catalyst under a wet etching environment without external bias.[7,8] The catalyst for MacEtch can be patterned by conventional techniques such as electron beam lithography followed by metal lift-off. Here we instead use a unique electrochemical stamping process (S4) for high throughput patterning of arbitrarily shaped nanoscale metallic materials[18,34] with feature sizes down to the 15−20 nm range. Stamps for S4 were written in Ag_2S using a FEI Dual Beam FIB. 30 nm of Ag was evaporated using a CHA evaporator on a clean piece of Si wafer. The resistivity of the p-type and n-type silicon wafers used is 6−8 and 1−10 Ωcm, respectively.

As illustrated in Figure 1, the inverse of the Ag_2S pattern was stamped into the Ag as the stamp is contacted to the Ag coated Si sample and a voltage is applied. Samples were etched in solutions containing various amounts of H_2O_2, HF, and EtOH for a period of 12 s to 6 min. When necessary, the Ag was removed using first a 7.5 min etch of H_2O_2/NH_4OH followed with a 5 min concentrated HNO_3 etch. After Ag removal, 12 nm of Ag was redeposited to study the plasmonic effect. Resulting nanostructures were characterized using a Hitachi S4800 SEM for morphology, and cathodoluminescence (CL) spectroscopy and imaging in a JEOL 7000F SEM for spatially resolved optical characterization at various stages including as etched, after Ag removal and Ag redeposition.

For TEM imaging, the nanowires were mechanically broken off from the substrate using a diamond scribe when the pattern containing desired nanowires was located using a precision stage and CCD camera. The broken nanowires were sonicated into solution and concentrated. A pipet was used to disperse the suspension of nanowires onto a holey carbon TEM grid. The JEOL LAB6 2010F and 2010FEG TEMs were used to acquire selected area diffraction (SAD) as well as high-resolution TEM images from the samples.

Acknowledgment. This work was supported by National Science Foundation under NSF Award no. 0749028 (CMMI) for The Center for Nanoscale Chemical-Electrical-Mechanical Manufacturing Systems, the NSF Career Award no. 0747178 (X.L.), and DOE award no. DEFG02-91-ER45439 for the TEM work.

REFERENCES AND NOTES

(1) Chan, C. K.; Peng, H. L.; Liu, G.; McIlwrath, K.; Zhang, X. F.; Huggins, R. A.; Cui, Y. *Nat. Nanotechnol.* **2008**, *3* (1), 31–35.
(2) Sinha, S.; Budhaev, B.; Majumdar, A. *Mater. Res. Soc. Symp. Proc.* **2009**, 1166.
(3) Hochbaum, A. I.; Chen, R. K.; Delgado, R. D.; Liang, W. J.; Garnett, E. C.; Najarian, M.; Majumdar, A.; Yang, P. D. *Nature* **2008**, *451* (7175), 163–U5.
(4) Tsakalakos, L.; Balch, J.; Fronheiser, J.; Korevaar, B. A.; Sulima, O.; Rand, J. *Appl. Phys. Lett.* **2007**, *91* (23), 233117.
(5) Tian, B.; Zheng, X.; Kempa, T. J.; Fang, Y.; Yu, N.; Yu, G.; Huang, J.; Lieber, C. M. *Nature* **2007**, *449* (7164), 885–889.
(6) Kalita, G.; Adhikari, S.; Aryal, H. R.; Afre, R.; Soga, T.; Sharon, M.; Koichi, W.; Umeno, M. *J. Phys. D: Appl. Phys.* **2009**, *42* (11), 115104.
(7) Garnett, E. C.; Yang, P. *J. Am. Chem. Soc.* **2008**, *130* (29), 9224–9225.
(8) Park, W. I.; Zheng, G.; Jiang, X.; Tian, B.; Lieber, C. M. *Nano Lett.* **2008**, *8* (9), 3004–3009.

© 2010 American Chemical Society

DOI: 10.1021/nl903841a | *Nano Lett.* **2010,** *10,* 1582--1588

(9) Choi, W. K.; Liew, T. H.; Dawood, M. K.; Smith, H. I.; Thompson, C. V.; Hong, M. H. *Nano Lett.* **2008**, *8* (11), 3799–3802.
(10) Chun, I. S.; Chow, E. K.; Li, X. *Appl. Phys. Lett.* **2008**, *92* (19), 191113–3.
(11) Canham, L. T. *Appl. Phys. Lett.* **1990**, *57* (10), 1046–1048.
(12) Belomoin, G.; Therrien, J.; Nayfeh, M. *Appl. Phys. Lett.* **2000**, *77* (6), 779–781.
(13) Gourbilleau, F.; Dufour, C.; Rezgui, B.; Brémond, G. *Mater. Sci. Eng., B* **2009**, *159*−*160*, 70–73.
(14) Zacharias, M.; Heitmann, J.; Scholz, R.; Kahler, U.; Schmidt, M.; Blasing, J. *Appl. Phys. Lett.* **2002**, *80* (4), 661–663.
(15) Saitow, K.; Yamamura, T. *J. Phys. Chem. C* **2009**, *113* (19), 8465–8470.
(16) Hadjersi, T.; Gabouze, N.; Yamamoto, N.; Benazzouz, C.; Cheraga, H. *Vacuum* **2005**, *80* (4), 366–370.
(17) Nayfeh, M. H.; Rao, S.; Nayfeh, O. M.; Smith, A.; Therrien, J. *IEEE Trans. Nanotechnol.* **2005**, *4* (6), 660–668.
(18) Hsu, K. H.; Schultz, P. L.; Ferreira, P. M.; Fang, N. X. *Nano Lett.* **2007**, *7* (2), 446–451.
(19) Schultz, P. L.; Hsu, K. H.; Fang, N. X.; Ferreira, P. M. *J. Vac. Sci. Technol., B* **2007**, *25* (6), 2419–2424.
(20) Li, X.; Bohn, P. W. *Appl. Phys. Lett.* **2000**, *77* (16), 2572–2574.
(21) Huang, Z.; Fang, H.; Zhu, J. *Adv. Mater.* **2007**, *19* (5), 744–748.
(22) Huang, Z. P.; Zhang, X. X.; Reiche, M.; Liu, L. F.; Lee, W.; Shimizu, T.; Senz, S.; Gosele, U. *Nano Lett.* **2008**, *8* (9), 3046–3051.
(23) Tsujino, K.; Matsumura, M. *Adv. Mater.* **2005**, *17* (8), 1045–1047.
(24) Kempa, T. J.; Tian, B.; Kim, D. R.; Hu, J.; Zheng, X.; Lieber, C. M. *Nano Lett.* **2008**, *8* (10), 3456–3460.
(25) Kandala, A.; Betti, T.; Morral, A. F. I. *Phys. Status Solidi A* **2009**, *206* (1), 173–178.
(26) Chang, S. W.; Chuang, V. P.; Boles, S. T.; Ross, C. A.; Thompson, C. V. *Adv. Funct. Mater.* **2009**, *19* (15), 2495–2500.
(27) Qu, Y.; Liao, L.; Li, Y.; Zhang, H.; Huang, Y.; Duan, X. *Nano Lett.*, submitted for publication.
(28) Hochbaum, A. I.; Gargas, D.; Hwang, Y. J.; Yang, P. *Nano Lett.*, submitted for publication.
(29) Zhang, M. L.; Peng, K. Q.; Fan, X.; Jie, J. S.; Zhang, R. Q.; Lee, S. T.; Wong, N. B. *J. Phys. Chem. C* **2008**, *112* (12), 4444–4450.
(30) Chattopadhyay, S.; Li, X.; Bohn, P. W. *J. Appl. Phys.* **2002**, *91* (9), 6134–6140.
(31) Zhao, Y.; Li, D. S.; Sang, W. B.; Yang, D. R.; Jiang, M. H. *Mod. Phys. Lett. B* **2008**, *22* (12), 1211–1220.
(32) Okamoto, K.; Niki, I.; Shvartser, A.; Narukawa, Y.; Mukai, T.; Scherer, A. *Nat. Mater.* **2004**, *3* (9), 601–605.
(33) Hui, F.; Xudong, L.; Shuang, S.; Ying, X.; Jing, Z. *Nanotechnology* **2008**, (25), 255703.
(34) Peter, L. S.; Keng, H. H.; Nicholas, X. F.; Placid, M. F. In Solid-state electrochemical nanoimprinting of copper; *J. Vac. Sci. Technol. B* **2007**, *25* (6), 2419−2424.

© 2010 American Chemical Society

DOI: 10.1021/nl903841a | *Nano Lett.* **2010,** *10,* 1582--1588